Relativistic electron dynamics in a cusped magnetic field with a downstream drift region

W. W. Destler, P. K. Misra, and M. J. Rhee

University of Maryland, College Park, Maryland 20742
(Received 10 February 1975; final manuscript received 18 August 1975)

Studies are reported of the motion of relativistic electrons injected first through a narrow magnetic cusp and then into a downstream region in which the particle motion is assumed to be adiabatic. Experiments performed to check the theory are also presented.

In a previous paper,[1] studies of the motion of relativistic electrons in cusped magnetic fields were reported. In general, electron or ion beam experiments employing cusped field geometries involve the injection of such beams first through a narrow magnetic cusp, and then into a downstream drift region in which the field gradients are sufficiently small so that the particle motion is essentially adiabatic.[2–5] The theoretical description discussed previously may easily be extended to describe particle motion in this case by solving the Lagrangian for the particle motion in the extended field. An infinitely small cusp transition is assumed and the magnetic field as a function of axial position z may be written,

$$B_z = B_0[1-(b+1)u], \tag{1a}$$

and accordingly

$$A_\theta = \frac{rB_0}{2}\,[1-(b+1)u], \tag{1b}$$

where u is the Heaviside step function, B_0 is the magnitude of the magnetic field on either side of the cusped field transition, and b is the downstream magnetic field normalized to B_0. In this case, b must satisfy the conditions

$$b = \begin{cases} 1 & \text{at } z = 0_+, \\ b(z) & \text{otherwise,} \end{cases}$$

where $b(z)$ is an arbitrary, well-behaved function with sufficiently small gradients so that the downstream particle motion may be assumed to be adiabatic. This idealized field is shown schematically in Fig. 1, along with the actual experimental field used to check the theory. A straightforward solution of the Lagrange equation for the z coordinate yields an expression for the axial velocity of the electron in the downstream region in terms of the initial velocity v_0 after acceleration in the diode, the upstream Larmor radius ρ_1, and b

$$v_{z_2}^2 = v_0^2 - \omega_c^2\, b(r_0^2+\rho_1^2)\,. \tag{2}$$

it is easily seen that in the case $b=1$, the previously reported results are obtained.

The maximum off-centering of particle orbits in the downstream field occurs for those particles with the largest upstream Larmor radius ρ_1. For a given par-

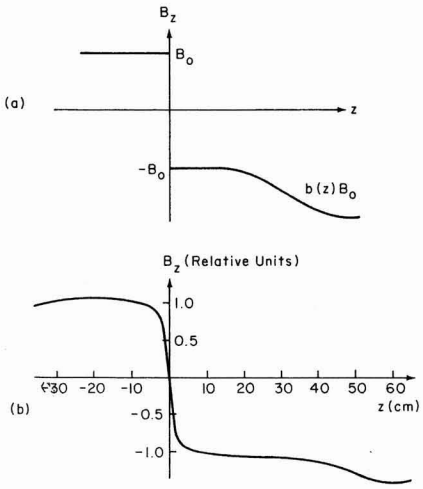

FIG. 1. Idealized (a) and experimental (b) cusp fields with adiabatically varying downstream drift regions.

ticle energy, ρ_1 will be greatest when v_{z_1} is exactly equal to the threshold velocity for transmission through the cusp and subsequent drift to the point z_0 in the downstream field. This threshold velocity is found by setting $v_{z_2}=0$ in Eq. (2), and, assuming the particle motion in the downstream field is adiabatic, yields an expression for the maximum particle off-centering ($R_{b\max}$) in the downstream field,

$$\frac{R_{b\max}^2}{r_0^2}=\frac{v_0^2}{\omega_c^2 b^2 r_0^2}-\frac{1}{b}\ . \tag{3}$$

In the manner described previously, this analysis may be used to construct a theoretical picture of the beam cross section as a function of time a distance z_0 downstream of the cusp transition. The time-of-flight from the cusp transition to the downstream observation point is given by

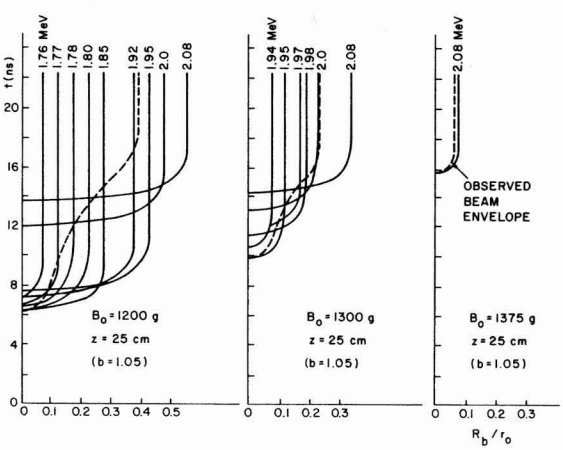

FIG. 2. Predicted arrival time of electrons at the observation point ($z_0=25$ cm) downstream of the cusp transition plotted as a function of the downstream offcentering of particle orbitals R_b, for several different electron energies. The observed beam envelope is shown to the same scale.

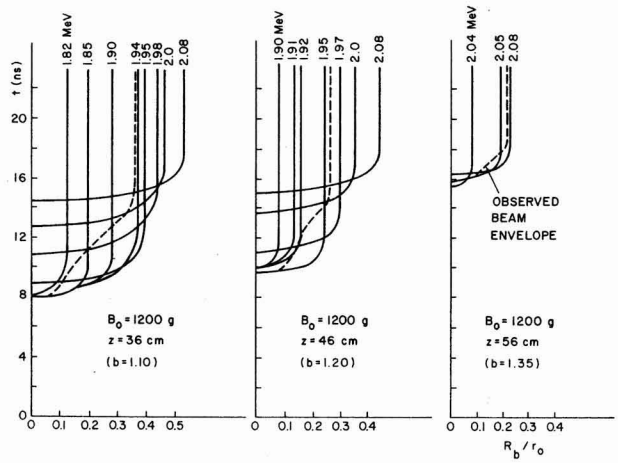

FIG. 3. Predicted and observed beam envelopes for constant B_0 and three different axial positions.

$$t_f=\int_0^{z_0}\frac{dz}{v_{z_2}},$$

where v_{z_2} is given by Eq. (2). If the departure time of an electron from the cusp transition is denoted by t_d, where t_d is determined empirically from the diode voltage waveform, then the electron will arrive at the observation point downstream of the cusp at a time given by $t=t_d+t_f$. Plots of this arrival time as a function of the downstream off-centering $R_b=\rho_1 b^{-1/2}$ (normalized to r_o) for $z_0=25$ cm (at this point, $b=1.05$) and several differ-

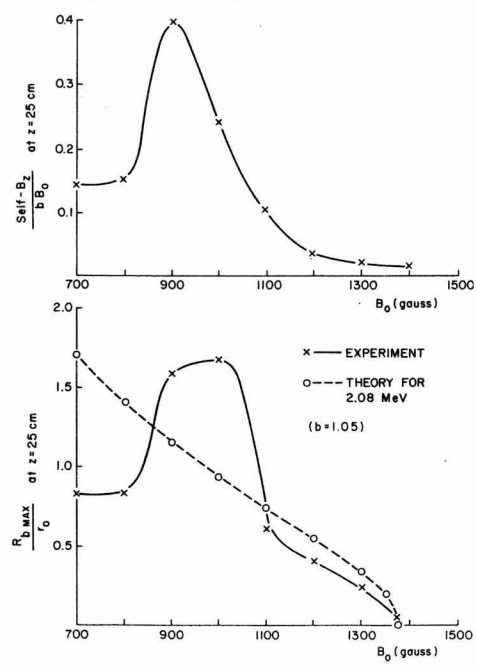

FIG. 4. Plot of the theoretically predicted and observed maximum downstream off-centering of particle orbits as a function of applied magnetic field. Also shown is the axial component of the self-magnetic field of the beam as a function of applied magnetic field at the same axial position.

ent electron energies have been constructed for $B_0 = 1200$, 1300, and 1375 G, and are shown in Fig. 2. As no restrictions have been placed on the possible magnitude of ρ_1 on the diode side of the cusp transition, other than the requirement that $\rho_1\omega_c$ not exceed v_o, the actual experimental data can be expected to lie somewhat inside the general profiles shown providing that the electrons follow single particle dynamics. Experimental results obtained using the scintillating rod technique described previously[1] are shown in the same figure for comparison. Similar experimental and theoretical downstream beam profiles have been constructed for the cases $B_0 = 1200$ G and $z_0 = 36$, 46, and 56 cm (corresponding to $b = 1.10$, and 1.20, and 1.35, respectively) and are shown in Fig. 3. Given the assumptions made in the first-order theoretical analysis, the experimental results are in reasonable agreement with theoretical expectations.

The maximum theoretically predicted beam width at the observation point is given by Eq. (3). Actual experimentally measured beam widths at any point in the downstream field can be expected to be less than or equal to this maximum value if the effect of the self-fields of the downstream beam on the particle dynamics can be neglected. Figure 4 shows this maximum beam width (normalized to r_0) at $z_0 = 25$ cm as a function of magnetic field for a 2.08 MeV electron beam. The actual peak diode voltage in the experiments was in the range 2.05 – 2.10 MV. Experimental data for the same conditions is shown for comparison. Also plotted in this figure is the ratio of the beam self-field (self-B_z) on axis to the externally applied field as measured with a fast integrated $\dot{B}$ probe. It can be seen that good agreement with the single particle theory can be found only for the case where the beam self-field is small compared with the applied field. Theoretical and experimental studies of the beam behavior under conditions where the self-fields of the beam are comparable to the applied fields are currently in progress.

This work was supported by the National Science Foundation under contract GP-29706.

[1]M. J. Rhee and W. W. Destler, Phys. Fluids **17**, 1574 (1974).
[2]C. A. Kapetanakos and W. M. Black, Bull. Am. Phys. Soc. **18**, 1264 (1973).
[3]R. E. Kribel, K. Shinsky, D. A. Phelps, and H. H. Fleischmann, Bull. Am. Phys. Soc. **17**, 999 (1972).
[4]M. P. Reiser, IEEE Trans. Nucl. Sci. NS-18, 460 (1971).
[5]M. P. Reiser, IEEE Trans. Nucl. Sci. NS-20, 310 (1973).